European Journal of Pharmaceutical Sciences 189 (2023) 106563

Contents lists available at ScienceDirect

European Journal of Pharmaceutical Sciences

journal homepage: www.elsevier.com/locate/ejps

In-line particle size measurement during granule fluidization using convolutional neural network-aided process imaging

Orsolya Péterfi [a], Lajos Madarász [a], Máté Ficzere [a], Katalin Lestyán-Goda [a], Petra Záhonyi [a], Gábor Erdei [b], Emese Sipos [c], Zsombor Kristóf Nagy [a,*], Dorián László Galata [a]

[a] Department of Organic Chemistry and Technology, Faculty of Chemical Technology and Biotechnology, Budapest University of Technology and Economics, Müegyetem rkp. 3., H-1111 Budapest, Hungary
[b] Department of Atomic Physics, Faculty of Natural Sciences, Budapest University of Technology and Economics, H-1111, Budapest, Budafoki 8, Hungary
[c] Department of Pharmaceutical Industry and Management, Faculty of Pharmacy, George Emil Palade University of Medicine, Pharmacy, Sciences and Technology of Targu Mures, Gheorghe Marinescu street 38, 540142 Targu Mures, Romania

ARTICLE INFO

Keywords:
Image analysis
Machine vision
Endoscope
Particle size distribution
Fluid-bed granulation
Convolutional neural networks

ABSTRACT

This paper presents a machine learning-based image analysis method to monitor the particle size distribution of fluidized granules. The key components of the direct imaging system are a rigid fiber-optic endoscope, a light source and a high-speed camera, which allow for real-time monitoring of the granules. The system was implemented into a custom-made 3D-printed device that could reproduce the particle movement characteristic in a fluidized-bed granulator. The suitability of the method was evaluated by determining the particle size distribution (PSD) of various granule mixtures within the 100–2000 μm size range. The convolutional neural network-based software was able to successfully detect the granules that were in focus despite the dense flow of the particles. The volumetric PSDs were compared with off-line reference measurements obtained by dynamic image analysis and laser diffraction. Similar trends were observed across the PSDs acquired with all three methods. The results of this study demonstrate the feasibility of performing real-time particle size analysis using machine vision as an in-line process analytical technology (PAT) tool.

1. Introduction

Fluidized-bed granulation is a process widely used in the pharmaceutical industry to improve powder properties for downstream processing. A number of processes, including homogenization, wetting, drying and particle size enlargement, are integrated into a single unit operation by using heat and mass transfer. As several processes are involved in this system, numerous process variables are known to influence the quality of the final product (Aulton and Summers, 2002; Burggraeve et al., 2013; Tan et al., 2006). Granule size and moisture content are considered the most critical aspects to control in the granulation process. The resulting particle size influences powder flowability, blend uniformity and tabletability, therefore monitoring particle size during granulation processes is of major importance (Du et al., 2014; Gabbott et al., 2016; Gao et al., 2002). The traditionally applied granulation control and endpoint determination tools are indirect, time-consuming and off-line testing methods, which do not ensure the consistent production of granules with the desired quality attributes (Fonteyne et al., 2015). This may lead to batch rejects and recalls, and requires continuous optimization of the granulation process.

Recently, the US Food and Drug Administration (FDA) has encouraged a shift from traditional off-line analysis to real-time quality assurance through the implementation of Process Analytical Technology (PAT) tools and Quality by Design (QbD) principles (*FDA, 2004*). Improved product quality can ultimately be achieved by identifying the critical material attributes (CMAs) and process parameters (CPPs), and understanding their effect on the critical quality attributes (CQAs) (Beg et al., 2019). PAT enables the identification and monitoring of these variables through a fast, non-invasive and non-destructive analysis. Thus, end-product quality, safety and efficacy is ensured by avoiding any process deviations during the manufacturing (Haneef and Beg, 2021). Near-infrared spectroscopy (NIR) (Findlay et al., 2005; Gavan et al., 2020; Nieuwmeyer et al., 2007), acoustic emission spectroscopy (Poutiainen et al., 2012; Tsujimoto et al., 2000), focused-beam reflectance spectroscopy (FBMR) (Alshihabi et al., 2013; Heath et al., 2002; Kukec et al., 2014) and spatial-filter velocimetry (SFV) (Burggraeve

* Corresponding author.
E-mail address: zsknagy@oct.bme.hu (Z.K. Nagy).

https://doi.org/10.1016/j.ejps.2023.106563
Received 12 May 2023; Received in revised form 24 July 2023; Accepted 12 August 2023
Available online 13 August 2023

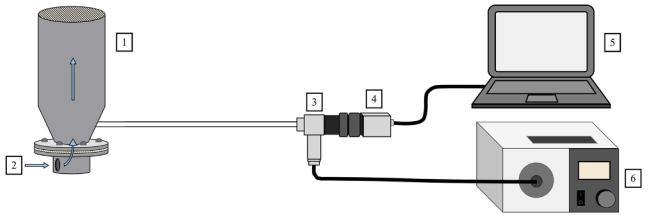

Fig. 1. Schematic drawing of the experimental setup: (1) 3D-printed mini-fluid, (2) fluidizing air, (3) rigid endoscope, (4) camera, (5) computer, (6) light source.

et al., 2010; Nascimento et al., 2021) have been used as in-line PAT tools for monitoring the fluid-bed granulation process.

Digital imaging is an affordable tool with enormous potential in many areas of the pharmaceutical industry (Galata et al., 2021). A digital imaging system consists of a digital camera capable of capturing images at a sufficiently high frames per second (fps) rate, the necessary optical components (i. e. lens, endoscope), a light source and algorithms to extract useful information from the images (Misra et al., 2015). Literature describes numerous methods to monitor particle size during granulation processes using various imaging techniques. An early attempt to capture pictures of granules during fluidized-bed granulation used an on-line particle image probe system consisting of a charge-coupled device (CCD) camera, a telephoto lens and a stroboscope (Watano et al., 1996; Watano and Miyanami, 1995). The first endoscopy-based particle imaging system was presented by Simon et al. for use in the crystallization process (Simon et al., 2009). Qian et al. (Qian et al., 2013) inserted a fiber-optic endoscope into a fluid-bed granulator to form motion images of the particles. In order to extract quantitative information from the captured pictures, the authors applied traditional image processing tools (filtering, denoising, binarization, segmentation). The performance of the aforementioned image analysis algorithms declines with dense material flow, because extensive granule overlap reduces the reliability of these methods. Furthermore, the changing image background, out-of-focus particles and rough granule surface often make segmentation more difficult (Larsen et al., 2006). The fluid bed is very dense at the bottom, especially towards the inlet slots (Fries et al., 2013); this presents major challenge for the traditional image analysis methods.

Photometric stereo imaging is a machine vision technique which can be used when the dispersion of particles is difficult. In this technique, multiple light sources are used to obtain 3D images of granules. Due to the nature of the measurement, the irregularities of rough particle surface could cast shades and a single particle may be regarded as multiple particles, consequently causing particle size underestimation (Heath et al., 2002; Sandler, 2011). This occurs especially in the case of irregular shaped granules and particle agglomeration (Silva et al., 2013; Soppela et al., 2011).

In recent years, artificial intelligence, and in particular convolutional neural networks (CNN), have made a great breakthrough in image-based object recognition. CNNs processes data of multiple dimensions, such as images, by using multiple building blocks: convolution layers, pooling layers, and fully connected layers. Convolution is applied to extract useful features from locally correlated data points. CNNs are designed to automatically and adaptively learn a large number of filters specific to a training dataset so that highly specific features can be detected anywhere on input images (Khan et al., 2020; Lopez Pinaya et al., 2019; Rawat and Wang, 2017). In the fields of pharmaceutical sciences, CNNs have shown outstanding performance and accuracy in the detection and characterization of powders (Sachs et al., 2023), crystal forms (Chen et al., 2019; Gan et al., 2022; Iwata et al., 2022; Salami et al., 2021), pellets (Mehle et al., 2017), tablets (Ma et al., 2020) and film coating (Ficzere et al., 2022; Hirschberg et al., 2020).

In the current work, a convolutional neural network-based in-line endoscopic system is proposed for particle size measurement. The system provides the opportunity to record and analyze images at rapid speed. In contrast to traditional detection algorithms where the detection rules are arbitrarily determined by a human, CNNs achieve robust and accurate performance by identifying the underlying patterns in the training dataset. Particle size measurement during fluidized-bed granulation is difficult due to the dense granule flow and particle overlap, therefore this work aims to investigate the feasibility of performing real-time particle size analysis using CNNs. To the authors knowledge, this is the first in-line granule size measurement method using an artificial intelligence-based endoscopic system during fluidization.

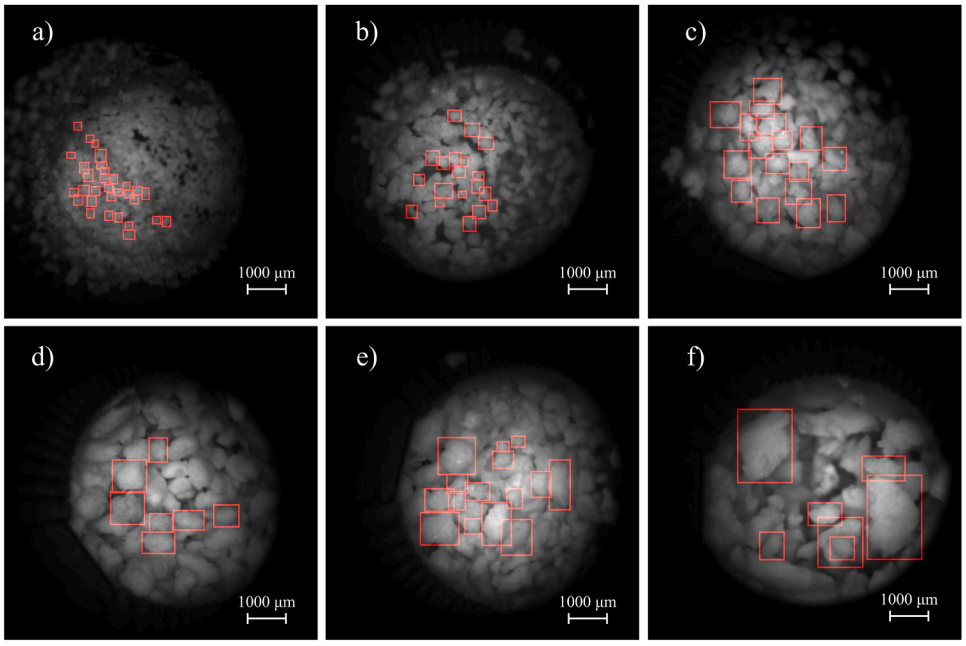

Fig. 2. Particle detection with V-CNN software using images of various dextrose granule fractions captured in the mini-fluid: (a) 200–300 µm, (b) 300–500 µm, (c) 500–710 µm, (d) 710–1000 µm, (e) 300–500 + 710–1000 µm, (f) 500–710 + 1000–2000 µm.

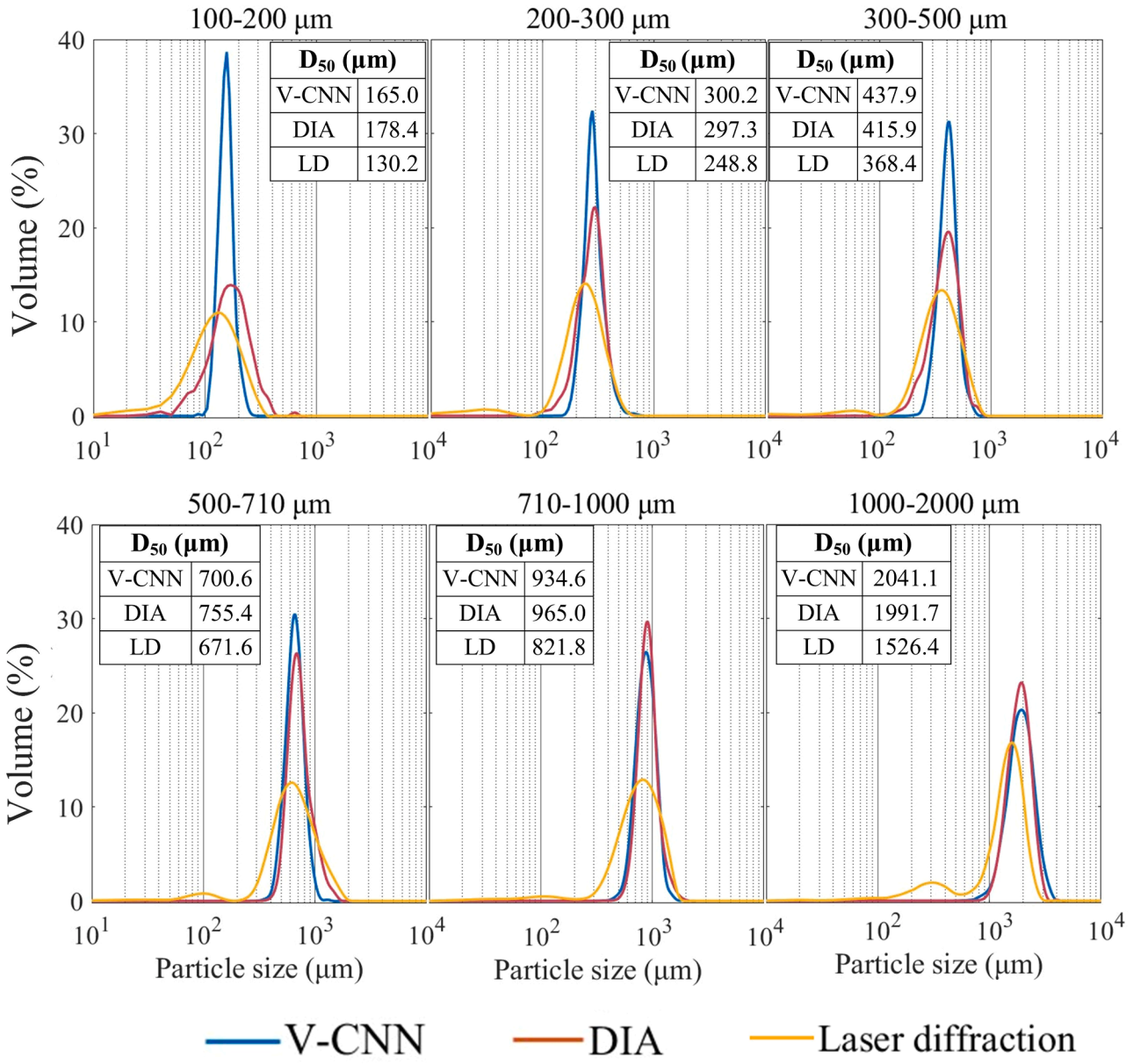

Fig. 3. The PSDs of the sieved dextrose granule fractions obtained with V-CNN, DIA and laser diffraction (LD).

2. Materials and methods

2.1. Materials

Dextrose granules were prepared with α-D glucose monohydrate (Hungrana, Hungary). Distilled water was used as granulation liquid. Starch-lactose granules contained polyvinylpyrrolidone (Kollidon® 30, PVPK30, BASF, Ludwigshafen, Germany) as binder, which was dissolved in 96% ethanol (Sigma-Aldrich, Budapest, Hungary). Potato starch (Roquette Pharma, Lestrem, France) and α-lactose monohydrate (GranuLac® 230 mesh, Meggle Pharma, Wasserburg, Germany) were used as the solid excipients.

2.2. Preparation of granules

Dextrose and starch-lactose granules were prepared using a previously studied continuous granulation system by Záhonyi et al. (Záhonyi et al., 2022). The obtained granules were sifted through 100, 200, 300, 500, 710, 1000 and 2000 µm sieves using a sieve shaker (CISA BA 200 N, Barcelona, Spain) with an amplitude of 2 mm until the mass of fractions no longer changed. Six fractions were obtained: 100–200 µm, 200–300 µm, 300–500 µm, 500–710 µm, 710–1000 µm and 1000–2000 µm. From the obtained fractions, five mixtures were prepared by mixing 10 g of smaller granule fractions with 10 g of large fractions: 300–500 + 500–710 µm, 300–500 + 710–1000 µm, 500–710 + 710–1000 µm, 500–710 + 1000–2000 µm and 710–1000 + 1000–2000 µm.

2.3. Experimental setup

A drawing of the experimental setup can be seen in Fig. 1. In this research, a custom-made 3D-printed device was used to simulate fluid bed granulation. The 3D model was designed in the Fusion 360 software. The device was printed on an Creality Ender 3 printer (Cordol Technology, Hong Kong) with polylactic acid (PLA) filament bobbin. The dimensions of mini-fluid were 160 mm in length and 60 mm in width. The device consisted of an upper and lower part connected through screws and separated by a filter, which allowed fluidizing airflow. The custom-made prototype described in this paper is available as

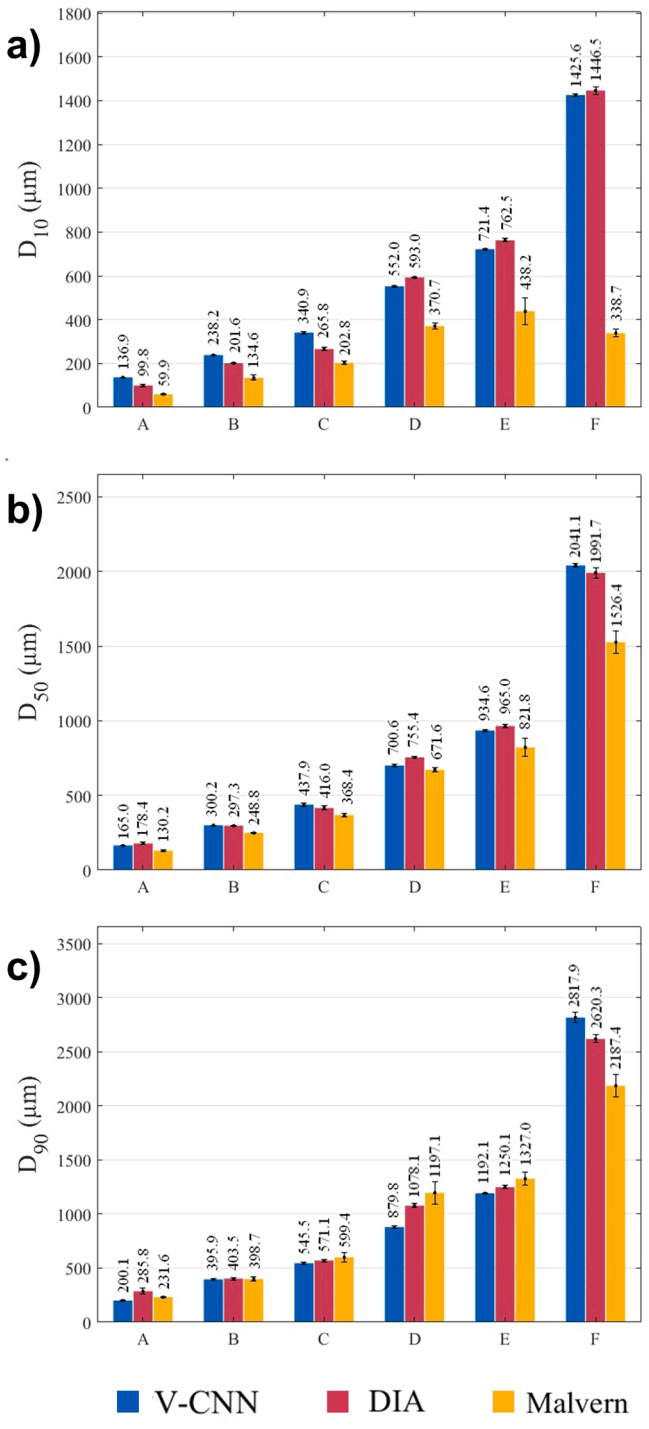

Fig. 4. Comparison between the D_{10}, D_{50} and D_{90} values of various dextrose granule fractions: 100–200 μm (A), 200–300 μm (B), 300–500 μm (C), 500–710 μm (D), 710–1000 μm (E), 1000–2000 μm (F).

supplementary material in standard tessellation language (STL) format. The granules were placed into the mini-fluid, then the top of the device was covered with a filter. A rigid endoscope of 5 mm diameter was inserted through the side of the 3D-printed device. The shell of the endoscope is made of stainless steel metal, with high hardness, making it suitable for pharmaceutical manufacturing processes. The endoscope was coupled with a high-powered LED light source through a fiber optic cable. All videos were acquired with a high-speed camera at 125 frames per second with a shutter speed of 85 μs. Video frame dimensions were cropped to 900 × 900 pixels. The pixel to μm ratio of the camera was determined using a caliper.

Image analysis was conducted using the CNN-based image analysis software (Videometry 1.2.2) software developed by QDevelopment (Budapest, Hungary), henceforth referred to as V-CNN. After recording the videos, we extracted individual video frames to create the dataset containing examples of the dextrose granules. For the training, we used 1.800 images with a total of 6.621 annotations of the granules that were in focus. Images were manually annotated using the Makesense on-line image annotation tool. The training data contained images of the six granule fractions and two of the mixtures (300–500 + 710–1000 μm and 500–710 + 1000–2000 μm). 10% of the images contained useless data (background, out-of-focus particles, partially visible granules), and therefore were not labelled. This ensures that the CNN will only detect the granules in focus, so that the particle size could be accurately determined. The dataset was split into 70% training and 30% testing set. The model was trained for 100 epochs in batch size of 15. After training, the model was used to perform image analysis on additional videos. Only dextrose granules were included in the training dataset, while testing was performed with both dextrose and starch-lactose granules. The average Feret-diameter of the granules was calculated in pixels, and then these values were converted to micrometers.

2.4. Off-line particle size analysis

The particle size of the granules was measured off-line by laser diffraction, using a Malvern Mastersizer 2000 (Malvern Instruments, Worcestershire, UK) and off-line dynamic image analysis based on the main principles of the Camsizer® particle size analyser, using a custom image analysis software previously presented by Madarász et al. The latter will be referred to as DIA (dynamic image analysis).

The laser diffraction technique uses Mie theory of light scattering to calculate the equivalent spherical diameter for non-spherical particles and gives their volumetric particle size distribution (PSD). 1 g of sample was fed into the device using a Malvern Scirocco 2000 feeding inlet. The measurement time was 6 s and dispersive air pressure was set to 1 bar.

The DIA technique determines the average Feret-diameter of the granules from the contours. The images of the particles were analyzed with a custom image analysis software developed by the authors. The following image processing methods have been implemented: gaussian blur, thresholding (binarization) and contouring (edge detection). The samples were fed into the measuring equipment using a vibratory feeder equipped with a U-shaped chute. The dispersed particles fell from the chute and passed between a custom panel light (Apokormat Ltd., Hungary) and a camera, which collected images of the sample stream. A Basler camera (Basler acA4112–30uc, Basler AG, Germany) was operated at 125 frames per second with a 1500 × 1050 resolution and a shutter speed of 200 μs.

The camera-based measurements allowed for the retrieval of the samples, while the Malvern Mastersizer is a destructive technique. Hence the measurement order for each sample was: V-CNN → DIA → Malvern. The sample was recollected between the measurements, in such a manner that the same material could be measured with each method. The measurements were repeated three times for each technique. The experimental data was expressed in volume-based distribution in order to ensure comparability.

3. Results and discussion

The images captured in the 3D-printed device are as shown in Fig. 2. Granule detection can be challenging due to the irregular particle surface, which casts shades on the rough surface. The V-CNN software was able to successfully detect the fully captured granules that were in focus and excluded the partially captured particles. Granules that were only partially in the frame or were covered by other granules, were not included in the training dataset as the true size of these granules could not be determined. This is because particle size estimation may be

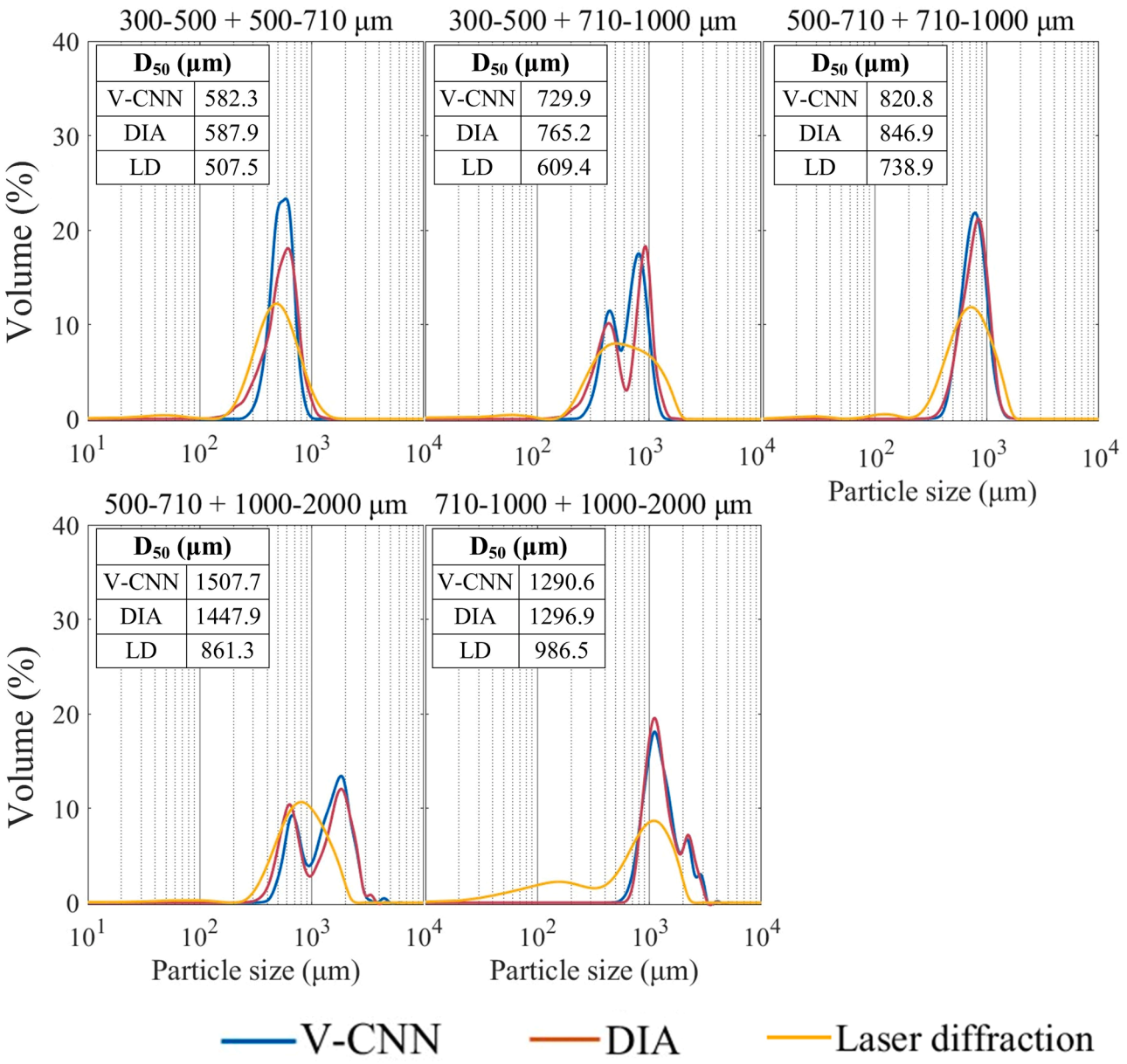

Fig. 5. The PSDs of the dextrose granule mixtures obtained with the different measurement techniques.

skewed when particles are only partially visible and large particles may be treated as smaller particles. A partially covered large granule was still annotated if the small particle did not influence the size of the annotation (i.e. it did not overlap with the contour of the large particle) and the particle size could be determined with sufficient accuracy (Fig. 2f.). Particles were correctly identified even though particle overlap was inevitable in the dense region of the fluid-bed. A video of the 500–710 µm granule fraction is available in the supplementary material of the article (Supplementary Video 1.).

Less light was reflected off of starch-lactose granules, which resulted in darker videos when the same camera settings were used. The gain was set to 3 dB for these granules to achieve similar detection rates. This value was enough to sufficiently amplify the apparent light sensitivity of the sensor with a minimal increase in noise.

The 100–2000 µm size range was considered as the fraction of interest as it corresponds with the typical range size of pharmaceutical granules. Granules with a similar size range were produced with fluidized-bed granulation in several literature works (Behzadi et al., 2005; Boerefijn and Hounslow, 2005; Hu et al., 2008; Närvänen et al., 2008). Granules smaller than 100 µm were not included in this study as it was not possible to visually determine which of these particles were in focus. The use of high-resolution magnifying endoscopes in combination with a zoom lens can improve video system magnification even further, allowing for the detection of smaller particles. Granules larger than 2000 µm were also recognized by the V-CNN software as seen in the PSD of the 1000–2000 µm sieve fraction. For larger particles it can be assumed that the system can be easily expanded upwards as long as the particles fit in the frame.

The surface of the endoscope remained clean even when small particles were present in the system. However, during wet granulation, materials may be sticky and adhesive, causing probe fouling and hindering in-line process monitoring. To address this issue, methods such as air purging, solvent rinsing, and the use of windshield wiping devices have been developed to mitigate probe fouling during measurement (Troup and Georgakis, 2013).

The PSDs were calculated from the size data of 5000 particles. The minimum number of particles required to be sampled can also be estimated using the sub-sampling method described by Clarke et al. (Clarke

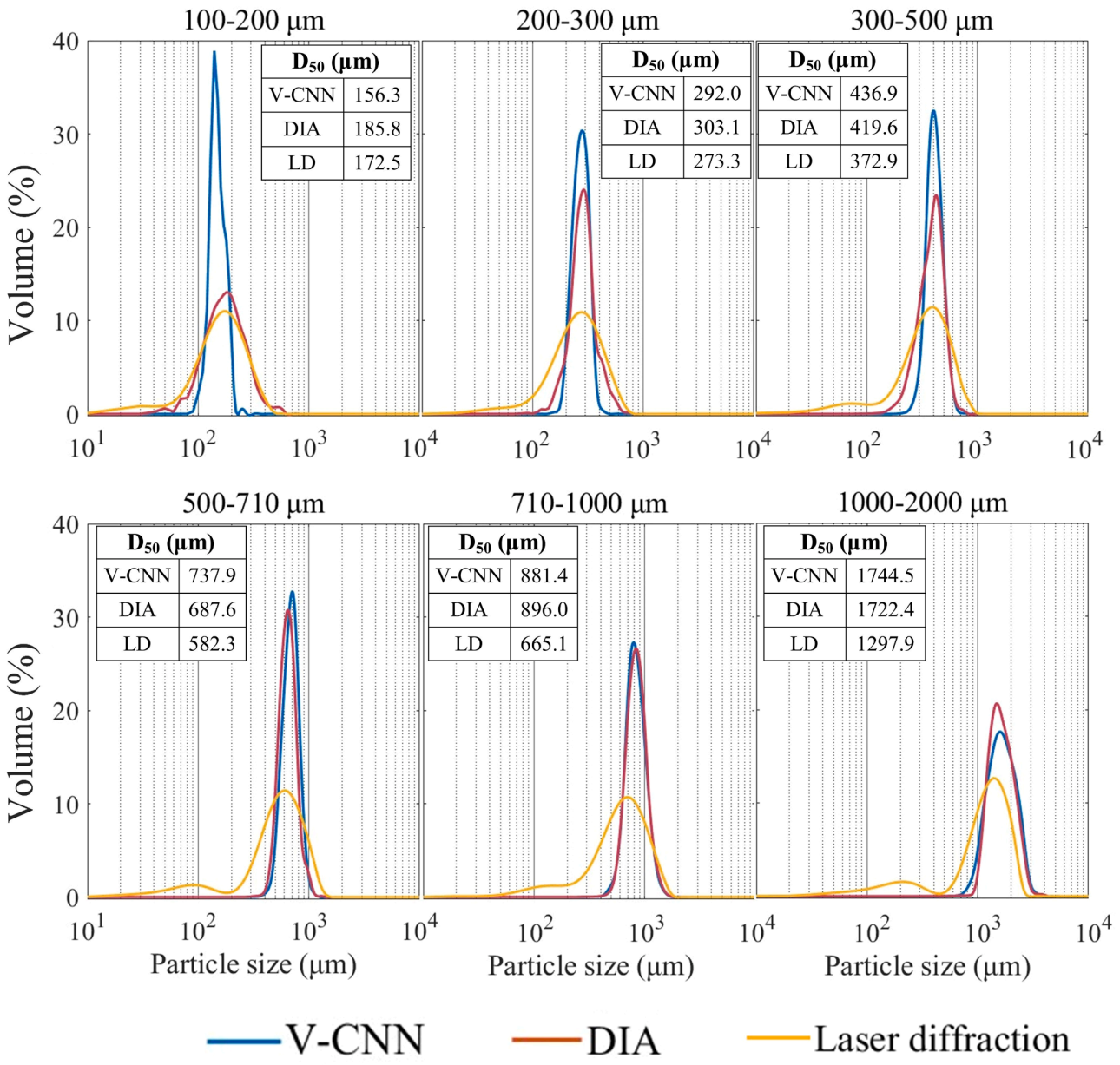

Fig. 6. The PSDs of the sieved starch-lactose granule fractions obtained with V-CNN, DIA and laser diffraction (LD).

et al., 2019). Since only a few particles can be observed in each frame, results were obtained after analyzing a few hundred to a few thousand frames depending on particle size. Determining the PSD of 1000–2000 µm granules required ~ 25 s as only a few larger granules could fit in one frame. The PSD of 300–500 µm and smaller granules could be determined in 4 s because ~10 granules were captured every frame. This shows that the measurement method is capable of monitoring fluid bed granulation in real-time, as changes in this process occur on a scale of several minutes.

Utilizing whole particle distributions can yield greater insight and provide deeper understanding of fundamental material properties (Gamble et al., 2023). The volume-based PSDs of the dextrose granule fractions are presented in Fig. 3. Similar trends were observed in PSDs across the different sizing techniques even if the absolute values varied. The camera-based approaches revealed a single peak of size distribution curve (unimodal) for sieved dextrose fractions. V-CNN measurements resulted in the narrowest distributions, closely followed by DIA. In contrast, the laser diffraction analysis was characterized by broad and multimodal distributions due to the increased percentage of smaller particles detected in the samples.

The average diameter (D_{10}, D_{50}, D_{90}) of the various dextrose granule fractions are represented in Fig. 4. The D_{10}, D_{50}, and D_{90} values are the specific particle diameters that correspond to the 10%, 50% and 90% of the total granules in the cumulative volume distribution.

Evaluation of the D_{10} values among the three methods revealed that the amount of small particles was found to be smaller with the camera-based methods and larger in the laser diffraction results. Mastersizer measurements indicated the presence of small granuleseven in the large granule fractions .

The mean particle size values obtained with the AI-based system showed good correlation with the offline DIA results, indicating that the developed model can perform accurate particle size measurements. The relative percentage difference between the D_{50} values measured with camera-based methods was less than 8% for all dextrose granule fractions.

The D_{50} values measured with laser diffraction were always lower than the camera-based measurements. These differences can be explained in part by the measurement methodology as the various

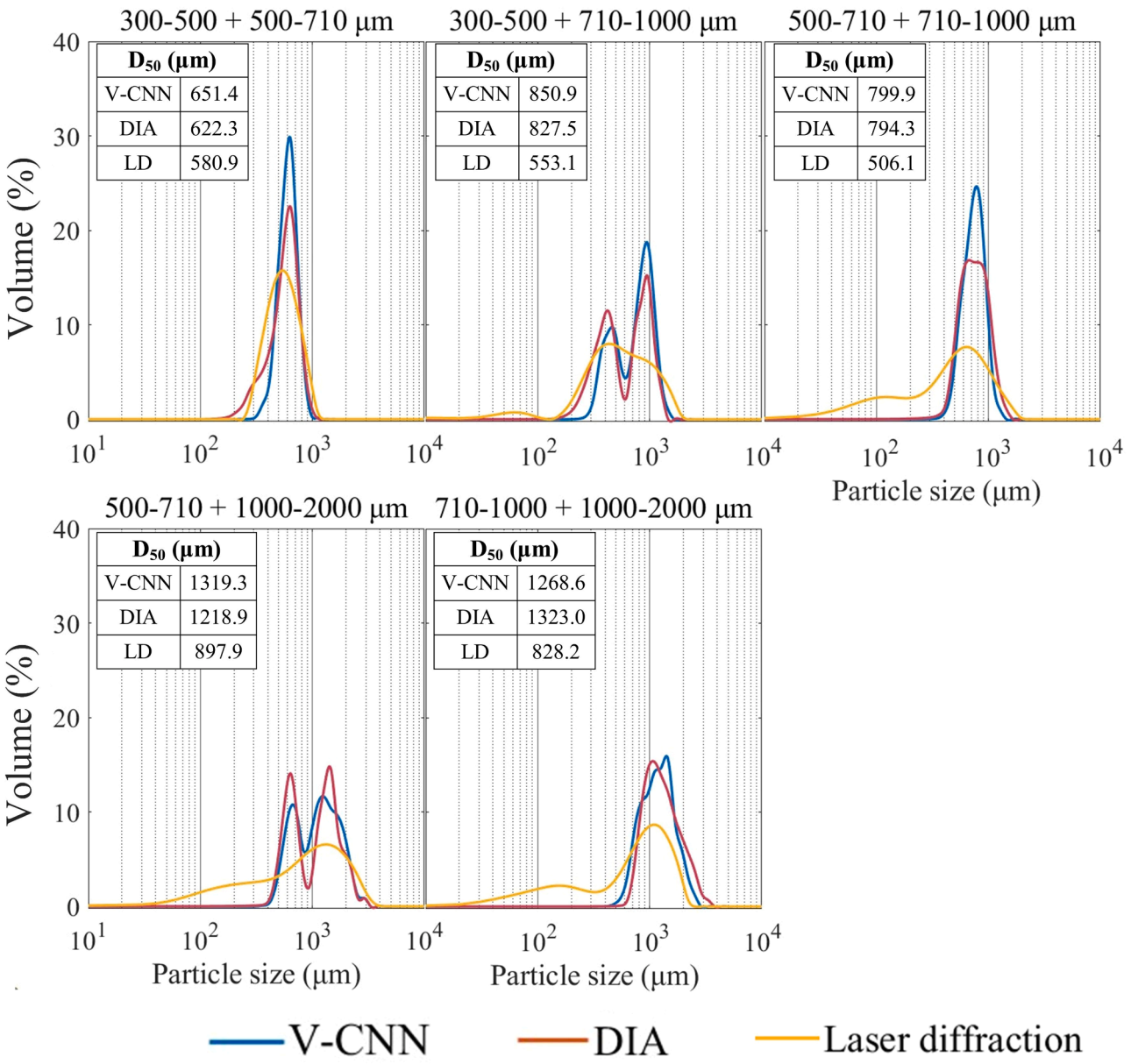

Fig. 7. The PSDs of the starch-lactose granule mixtures obtained with the different measurement techniques.

measurement techniques handle particle shape differently. As presented in several papers comparing particle size measurement methods, this phenomenon has been observed mainly with irregularly shaped particles (Grubbs et al., 2021; Islam et al., 2022; Li et al., 2005; Roostaei et al., 2020; Silva et al., 2013).

The comparison between the PSDs of the various dextrose granule mixtures are depicted in Fig. 5. Three mixtures prepared with sieved granule fractions (300–500 + 710–1000 µm, 500–710 + 1000–2000 µm, 710–1000 + 1000–2000 µm) showed bimodal distributions. This bimodality was not visible with the Mastersizer measurements, which may be due to instrumental corrections such as smoothing of the PSD profile during data processing (Blott and Pye, 2006). It should be noted that even though the same amount of granule fractions were mixed during sample preparation, mass distribution would not be completely comparable with the volume size distribution if the porosity and density of the granules varied.

A well-trained machine learning model is able to generalize so that it can accurately detect similar objects in previously unseen input data. We assessed the suitability of the AI-based technique on fresh data by applying the method to starch-lactose granules. The PSDs of the assayed starch-lactose granule fractions and mixtures (Fig. 6. and 7.) show that the distributions determined with camera-based methods corresponded well with the size fraction ranges of the sieved granules despite the CNN model being trained on dextrose granules. Bimodal distribution was observed with camera-based methods for two mixtures prepared with nonadjacent sieve fractions (300–500 + 710–1000 µm and 500–710 + 1000–2000 µm), as was anticipated. The AI-based system was able to determine the particle size of the starch-lactose granules with similar accuracy as the dextrose granules. The average relative standard deviation values calculated for D_{50} values with V-CNN, DIA and laser diffraction were 1.1%, 2.8% and 4.1% for dextrose granules and 1.0%, 3.8% and 4.4% for starch-lactose granules.

Mastersizer results indicate the presence of 100–400 µm particles in the 1000–2000 µm fraction, however these small particles were not detected with the camera-based methods. This is also reflected by the span values which show a wide variance between the three methods. Laser diffraction measurements produced the widest distributions, whereas the small span values measured with the AI-based system

indicate a narrow PSD. The span values of the DIA method were between the two techniques, but much closer to that of V-CNN.

All three particle sizing techniques showed similar tendency in the D_{50} values of the starch-lactose granules. For all granule fractions and mixtures within the 200–2000 μm size range the relative percentage difference between the mean particle size values measured with V-CNN and DIA was less than 8%. This difference was 17.2% in the case of the 100–200 μm granules.

Overall, the PSDs of the various granule fractions and mixtures indicate that there is a systematic difference between the camera-based techniques and the laser diffraction data. The most remarkable difference was observed in the smallest fraction, which was larger in the Mastersizer results. This effect was more prominent with large starch-lactose granules. The CNN model performed similarly well for both dextrose and starch-lactose granules, demonstrating that the AI was able to learn the generalized features of the granules. Additional data on the D_{10}, D_{50}, D_{90} and span values of the other samples are available in the supplementary material (Supplementary Figure 1–5.).

4. Conclusion

An endoscope can be easily integrated onto most fluidized-bed granulators with no modification of the equipment, by mounting within the sampling port. The AI-based imaging system can ultimately be used as an in-line sensor to monitor granulation process and detect end-point. This work evaluates the suitability of an artificial intelligence-based endoscopic system for measuring particle size distribution during fluidization.

The endoscopic system was tested in a laboratory setting with a custom-made 3D-printed device that simulated the particle movement during fluid bed granulation. Images of the granules were successfully retrieved and particles were detected despite the dense flow of the particles. Granules from both batches were recognized by the trained model even though only dextrose granules were included in the training dataset. The model was also able to distinguish between blurry and in-focus particles. The performance of the technique was evaluated by comparing the obtained PSDs to two off-line reference measurement methods (laser diffraction and off-line dynamic image analysis). The developed imaging system seems promising; the results of this initial study demonstrate a good relationship between in-line and off-line measurement of granule size. The result of the three methods showed similar trends in the PSDs, however the different measurement principles resulted in different mean particle sizes. The AI-based system employs cost-effective instrumentation; however validation costs should also be considered in a pharmaceutical setting. The system offers flexibility by supporting various combinations of endoscopes and cameras, thereby enabling extensive customization.

Our conclusion is that the developed AI-based endoscopic system is highly feasible as a PAT tool for monitoring particle fluidization. In future work, the video system magnification can be improved through the optimization of the optics. As a continuation of the research, the method should be tested in an industrial setting during fluid-bed granulation.

Declaration of Competing Interest

The authors declare that they have no known competing financial interests or personal relationships that could have appeared to influence the work reported in this paper.

Data availability

Data will be made available on request.

Acknowledgements

Project no. RRF-2.3.1–21–2022–00015 has been implemented with the support provided by the European Union. The research has been implemented with the support provided by the Ministry of Innovation and Technology of Hungary from the National Research, Development and Innovation Fund, financed under the [K-143039] funding scheme. This project was supported by the ÚNKP-22–4-II-BME-137 New National Excellence Program of the Ministry of Human Capacities. The authors would like to thank Szabolcs Mihály for his support provided in the data analysis.

Supplementary materials

Supplementary material associated with this article can be found, in the online version, at doi:10.1016/j.ejps.2023.106563.

References

Alshihabi, F., Vandamme, T., Betz, G., 2013. Focused beam reflectance method as an innovative (PAT) tool to monitor in-line granulation process in fluidized bed. Pharm. Dev. Technol. 18, 73–84. https://doi.org/10.3109/10837450.2011.627868.

Aulton, M.E., Summers, M., 2002. Granulation. In: Aulton, M.E. (Ed.), PharmaceuticsThe Science of Dosage Form Design. Elsevier Limited, Churchill Livingstone, pp. 364–378.

Beg, S., Hasnain, M.S., Rahman, M., Swain, S., 2019. Introduction to Quality by Design (QbD): Fundamentals, Principles, and Applications, Pharmaceutical Quality By Design. Elsevier Inc. https://doi.org/10.1016/b978-0-12-815799-2.00001-0.

Behzadi, S.S., Klocker, J., Hüttlin, H., Wolschann, P., Viernstein, H., 2005. Validation of fluid bed granulation utilizing artificial neural network. Int. J. Pharm. 291, 139–148. https://doi.org/10.1016/j.ijpharm.2004.07.051.

Blott, S.J., Pye, K., 2006. Particle size distribution analysis of sand-sized particles by laser diffraction: An experimental investigation of instrument sensitivity and the effects of particle shape. Sedimentology 53, 671–685. https://doi.org/10.1111/j.1365-3091.2006.00786.x.

Boerefijn, R., Hounslow, M.J., 2005. Studies of fluid bed granulation in an industrial R&D context. Chem. Eng. Sci. 60, 3879–3890. https://doi.org/10.1016/j.ces.2005.02.021.

Burggraeve, A., Monteyne, T., Vervaet, C., Remon, J.P., Beer, T.De, 2013. Process analytical tools for monitoring, understanding, and control of pharmaceutical fluidized bed granulation: A review. Eur. J. Pharm. Biopharm. 83, 2–15. https://doi.org/10.1016/j.ejpb.2012.09.008.

Burggraeve, A., Van Den Kerkhof, T., Hellings, M., Remon, J.P., Vervaet, C., De Beer, T., 2010. Evaluation of in-line spatial filter velocimetry as PAT monitoring tool for particle growth during fluid bed granulation. Eur. J. Pharm. Biopharm. 76, 138–146. https://doi.org/10.1016/j.ejpb.2010.06.001.

Chen, S., Liu, T., Xu, D., Huo, Y., Yang, Y., 2019. Image based measurement of population growth rate for l-glutamic acid crystallization. Chinese Control Conf. CCC 2019-July, 7933–7938. doi:10.23919/ChiCC.2019.8866441.

Clarke, J., Gamble, J.F., Jones, J.W., Tobyn, M., Greenwood, R., Ingram, A., 2019. Alternative approach for defining the particle population requirements for static image analysis based particle characterization methods. Adv. Powder Technol. 30, 920–929. https://doi.org/10.1016/j.apt.2019.02.006.

Du, P., Du, J., Smyth, H.D.C., 2014. Evaluation of Granulated Lactose as a Carrier for DPI Formulations 1: Effect of Granule Size. Ageing Int. 15, 1417–1428. https://doi.org/10.1208/s12249-014-0166-z.

Ficzere, M., Mészáros, L.A., Kállai-Szabó, N., Kovács, A., Antal, I., Nagy, Z.K., Galata, D. L., 2022. Real-time coating thickness measurement and defect recognition of film coated tablets with machine vision and deep learning. Int. J. Pharm. 623 https://doi.org/10.1016/j.ijpharm.2022.121957.

Findlay, W.P., Peck, G.R., Morris, K.R., 2005. Determination of fluidized bed granulation end point using near-infrared spectroscopy and phenomenological analysis. J. Pharm. Sci. 94, 604–612. https://doi.org/10.1002/jps.20276.

Fonteyne, M., Vercruysse, J., De Leersnyder, F., Van Snick, B., Vervaet, C., Remon, J.P., De Beer, T., 2015. Process Analytical Technology for continuous manufacturing of solid-dosage forms. TrAC - Trends Anal. Chem. 67, 159–166. https://doi.org/10.1016/j.trac.2015.01.011.

Fries, L., Antonyuk, S., Heinrich, S., Dopfer, D., Palzer, S., 2013. Collision dynamics in fluidised bed granulators: A DEM-CFD study. Chem. Eng. Sci. 86, 108–123. https://doi.org/10.1016/j.ces.2012.06.026.

Gabbott, I.P., Al Husban, F., Reynolds, G.K., 2016. The combined effect of wet granulation process parameters and dried granule moisture content on tablet quality attributes. Eur. J. Pharm. Biopharm. 106, 70–78. https://doi.org/10.1016/j.ejpb.2016.03.022.

Galata, D.L., Mészáros, L.A., Kállai-Szabó, N., Szabó, E., Pataki, H., Marosi, G., Nagy, Z. K., 2021. Applications of machine vision in pharmaceutical technology: A review. Eur. J. Pharm. Sci. 159 https://doi.org/10.1016/j.ejps.2021.105717.

Gamble, J.F., Akseli, I., Ferreira, A.P., Leane, M., Thomas, S., Tobyn, M., Wadams, R.C., 2023. Morphological distribution mapping: Utilisation of modelling to integrate

particle size and shape distributions. Int. J. Pharm. 635, 122743 https://doi.org/10.1016/j.ijpharm.2023.122743.
Gan, C., Wang, L., Xiao, S., Zhu, Y., 2022. Feedback Control of Crystal Size Distribution for Cooling Batch Crystallization Using Deep Learning-Based Image Analysis. Crystals 12. https://doi.org/10.3390/cryst12050570.
Gao, J.Z.H., Jain, A., Motheram, R., Gray, D.B., Hussain, M.A., 2002. Fluid bed granulation of a poorly water soluble, low density, micronized drug: Comparison with high shear granulation. Int. J. Pharm. 237, 1–14. https://doi.org/10.1016/S0378-5173(01)00982-6.
Gavan, A., Iurian, S., Casian, T., Porfire, A., Porav, S., Voina, I., Oprea, A., Tomuta, I., 2020. Fluidised bed granulation of two APIs: QbD approach and development of a NIR in-line monitoring method. Asian J. Pharm. Sci. 15, 506–517. https://doi.org/10.1016/j.ajps.2019.03.003.
Grubbs, J., Tsaknopoulos, K., Massar, C., Young, B., O'Connell, A., Walde, C., Birt, A., Siopis, M., Cote, D., 2021. Comparison of laser diffraction and image analysis techniques for particle size-shape characterization in additive manufacturing applications. Powd. Technol. 391, 20–33. https://doi.org/10.1016/j.powtec.2021.06.003.
Haneef, J., Beg, S., 2021. Quality by design-based development of nondestructive analytical techniques. In: Beg, Sarwar, Md Saquib Hasnain, Mahfoozur, Rahman, W. H.A. (Eds.), Handbook of Analytical Quality By Design. Academic Press, pp. 153–166. https://doi.org/10.1016/B978-0-12-820332-3.00006-6.
Heath, A.R., Fawell, P.D., Bahri, P.A., Swift, J.D., 2002. Estimating average particle size by focused beam reflectance measurement (FBRM). Part. Part. Syst. Charact. 19, 84–95. https://doi.org/10.1002/1521-4117(200205)19:2<84::AID-PPSC84>3.0.CO;2-1.
Hirschberg, C., Edinger, M., Holmfred, E., Rantanen, J., Boetker, J., 2020. Image-based artificial intelligence methods for product control of tablet coating quality. Pharmaceutics 12, 1–9. https://doi.org/10.3390/pharmaceutics12090877.
Hu, X., Cunningham, J.C., Winstead, D., 2008. Study growth kinetics in fluidized bed granulation with at-line FBRM. Int. J. Pharm. 347, 54–61. https://doi.org/10.1016/j.ijpharm.2007.06.043.
Islam, S.F., Hawkins, S.M., Meyer, J.L.L., Sharman, A.R.C., 2022. Evaluation of different particle size distribution and morphology characterization techniques. Addit. Manuf. Lett. 3, 100077 https://doi.org/10.1016/j.addlet.2022.100077.
Iwata, H., Hayashi, Y., Hasegawa, A., Terayama, K., Okuno, Y., 2022. Classification of scanning electron microscope images of pharmaceutical excipients using deep convolutional neural networks with transfer learning. Int. J. Pharm. X 4, 100135. https://doi.org/10.1016/j.ijpx.2022.100135.
Khan, A., Sohail, A., Zahoora, U., Qureshi, A.S., 2020. A Survey of the Recent Architectures of Deep Convolutional Neural networks, Artificial Intelligence Review. Springer, Netherlands. https://doi.org/10.1007/s10462-020-09825-6.
Kukec, S., Hudovornik, G., Dreu, R., Vrečer, F., 2014. Study of granule growth kinetics during in situ fluid bed melt granulation using in-line FBRM and SFT probes. Drug Dev. Ind. Pharm. 40, 952–959. https://doi.org/10.3109/03639045.2013.791832.
Larsen, P.A., Rawlings, J.B., Ferrier, N.J., 2006. An algorithm for analyzing noisy, in situ images of high-aspect-ratio crystals to monitor particle size distribution. Chem. Eng. Sci. 61, 5236–5248. https://doi.org/10.1016/j.ces.2006.03.035.
Li, M., Wilkinson, D., Patchigolla, K., 2005. Comparison of particle size distributions measured using different techniques. Part. Sci. Technol. 23, 265–284. https://doi.org/10.1080/02726350590955912.
Lopez Pinaya, W.H., Vieira, S., Garcia-Dias, R., Mechelli, A., 2019. Convolutional neural networks. Machine Learning: Methods and Applications to Brain Disorders. Elsevier Inc. https://doi.org/10.1016/B978-0-12-815739-8.00010-9.
Ma, X., Kittikunakorn, N., Sorman, B., Xi, H., Chen, A., Marsh, M., Mongeau, A., Piché, N., Williams, R., Skomski, D., 2020. Deep Learning Convolutional Neural Networks for Pharmaceutical Tablet Defect Detection. Microsc. Microanal. 26, 1606–1609. https://doi.org/10.1017/S1431927620018693.
Mehle, A., Likar, B., Tomaževič, D., 2017. In-line recognition of agglomerated pharmaceutical pellets with density-based clustering and convolutional neural network. IPSJ Trans. Comput. Vis. Appl. 9, 2–7. https://doi.org/10.1186/s41074-017-0019-2.
Misra, N.N., Sullivan, C., Cullen, P.J., 2015. Process Analytical Technology (PAT) and Multivariate Methods for Downstream Processes. Curr. Biochem. Eng. 2, 4–16. https://doi.org/10.2174/2213385203666150219231836.
Närvänen, T., Lipsanen, T., Antikainen, O., Räikkönen, H., Yliruusi, J., 2008. Controlling granule size by granulation liquid feed pulsing. Int. J. Pharm. 357, 132–138. https://doi.org/10.1016/j.ijpharm.2008.01.060.
Nascimento, R.F., Ávila, M.F., Taranto, O.P., Kurozawa, L.E., 2021. A new approach to the mechanisms of agglomeration in fluidized beds based on Spatial Filter Velocimetry measurements. Powd. Technol. 393, 219–228. https://doi.org/10.1016/j.powtec.2021.07.076.
Nieuwmeyer, F.J.S., Damen, M., Gerich, A., Rusmini, F., Van Der Voort Maarschalk, K., Vromans, H., 2007. Granule characterization during fluid bed drying by development of a near infrared method to determine water content and median granule size. Pharm. Res. 24, 1854–1861. https://doi.org/10.1007/s11095-007-9305-5.
Poutiainen, S., Matero, S., Hämäläinen, T., Leskinen, J., Ketolainen, J., Järvinen, K., 2012. Predicting granule size distribution of a fluidized bed spray granulation process by regime based PLS modeling of acoustic emission data. Powd. Technol. 228, 149–157. https://doi.org/10.1016/j.powtec.2012.05.010.
Qian, L., Lu, Y., Zhong, W., Chen, X., Ren, B., Jin, B., 2013. Developing a novel fibre high speed photography method for investigating solid volume fraction in a 3D spouted bed. Can. J. Chem. Eng. 91, 1793–1799. https://doi.org/10.1002/cjce.21915.
Rawat, W., Wang, Z., 2017. Deep Convolutional Neural Networks for Image Classification: A Comprehensive Review. Neural Comput. 29, 2352–2449. https://doi.org/10.1162/NECO_a_00990.
Roostaei, M., Reservoir, R.G.L., Hosseini, S.A., 2020. Comparison of Various Particle-Size Distribution-Measurement Methods. Paper presented at the SPE International Conference and Exhibition on Formation Damage Control, Lafayette, Louisiana, USA, 19–21. doi:10.2118/199335-MS.
Sachs, S., Ratz, M., Mäder, P., König, J., Cierpka, C., 2023. Particle detection and size recognition based on defocused particle images: a comparison of a deterministic algorithm and a deep neural network. Exp. Fluids 64, 1–16. https://doi.org/10.1007/s00348-023-03574-2.
Salami, H., McDonald, M.A., Bommarius, A.S., Rousseau, R.W., Grover, M.A., 2021. Situ Imaging Combined with Deep Learning for Crystallization Process Monitoring: Application to Cephalexin Production. Org. Process Res. Dev. 25, 1670–1679. https://doi.org/10.1021/acs.oprd.1c00136.
Sandler, N., 2011. Photometric imaging in particle size measurement and surface visualization. Int. J. Pharm. 417, 227–234. https://doi.org/10.1016/j.ijpharm.2010.11.007.
Silva, A.F.T., Burggraeve, A., Denon, Q., Van Der Meeren, P., Sandler, N., Van Den Kerkhof, T., Hellings, M., Vervaet, C., Remon, J.P., Lopes, J.A., De Beer, T., 2013. Particle sizing measurements in pharmaceutical applications: Comparison of in-process methods versus off-line methods. Eur. J. Pharm. Biopharm. 85, 1006–1018. https://doi.org/10.1016/j.ejpb.2013.03.032.
Simon, L.L., Nagy, Z.K., Hungerbuhler, K., 2009. Endoscopy-based in situ bulk video imaging of batch crystallization processes. Org. Process Res. Dev. 13, 1254–1261. https://doi.org/10.1021/op900019b.
Soppela, I., Airaksinen, S., Hatara, J., Räikkönen, H., Antikainen, O., Yliruusi, J., Sandler, N., 2011. Rapid particle size measurement using 3D surface imaging. AAPS PharmSciTech 12, 476–484. https://doi.org/10.1208/s12249-011-9607-0.
Tan, H.S., Salman, A.D., Hounslow, M.J., 2006. Kinetics of fluidised bed melt granulation I: The effect of process variables. Chem. Eng. Sci. 61, 1585–1601. https://doi.org/10.1016/j.ces.2005.09.012.
Troup, G.M., Georgakis, C., 2013. Process systems engineering tools in the pharmaceutical industry. Comput. Chem. Eng. 51, 157–171. https://doi.org/10.1016/j.compchemeng.2012.06.014.
Tsujimoto, H., Yokoyama, T., Huang, C.C., Sekiguchi, I., 2000. Monitoring particle fluidization in a fluidized bed granulator with an acoustic emission sensor. Powd. Technol. 113, 88–96. https://doi.org/10.1016/S0032-5910(00)00205-9.
U.S. Food and Drug Administration, 2004. Guidance For Industry. PAT- a framework For Innovative Pharmaceutical development, Manufacturing and Quality Assurance. Silver Spring, MD: FDA. Available from. https://www.fda.gov/media/71012/download (Acccessed: 13 March 2023).
Watano, S., Miyanami, K., 1995. Image processing for on-line monitoring of granule size distribution and shape in fluidized bed granulation. Powd. Technol. 83, 55–60. https://doi.org/10.1016/0032-5910(94)02944-J.
Watano, S., Sato, Y., Miyanami, K., 1996. Control of Granule Growth in Fluidized Bed Granulation by an Image Processing System. Chem. Pharm. Bull. 44, 1556–1560. https://doi.org/10.1248/cpb.44.1556.
Záhonyi, P., Szabó, E., Domokos, A., Haraszti, A., Gyürkés, M., Moharos, E., Nagy, Z.K., 2022. Continuous integrated production of glucose granules with enhanced flowability and tabletability. Int. J. Pharm. 626 https://doi.org/10.1016/j.ijpharm.2022.122197.